Experimental Evidence for a Zigzag Bifurcation in Bulk Lamellar Eutectic Growth

Silvère Akamatsu, Sabine Bottin-Rousseau,* and Gabriel Faivre

Groupe de Physique des Solides, CNRS UMR 7588, Universités Pierre-et-Marie-Curie et Denis-Diderot, Campus Boucicaut, 140 rue de Lourmel, 75015 Paris, France

(Received 13 July 2004; published 20 October 2004)

We present real-time observations of the directional-solidification patterns of a transparent nonfaceted eutectic alloy (CBr_4-C_2Cl_6) in bulk samples. The growth front of the two-phase solid is observed from the top through the liquid and the glass wall of the container with a long-distance microscope. We show that, in near-eutectic CBr_4-C_2Cl_6 alloys, the upper stability limit of the stationary lamellar patterns is due to a zigzag bifurcation, which occurs at an interlamellar spacing of about $0.85\lambda_m$, where λ_m is the minimum-undercooling spacing. The zigzag patterns undergo a lamella breakup instability leading to the creation of new lamellae at about $1.1\lambda_m$. On the other hand, the lower stability limit of the stationary patterns is due to the same instability as in thin samples, namely, a lamella termination instability that occurs at about $0.7\lambda_m$.

DOI: 10.1103/PhysRevLett.93.175701 PACS numbers: 64.70.Dv, 05.70.Ln, 81.30.Fb

Nonlinear pattern formation in solidification is a question of general interest in the physics of spatially extended out-of-equilibrium systems [1]. Solidification patterns or "microstructures" are also the subject of active researches in materials sciences [2]. One of the most frequently studied examples is that of directionally solidified (solidified at a fixed velocity V in an applied unidirectional thermal gradient), nonfaceted binary eutectics (two-component alloys presenting a miscibility gap in the solid state). For thermodynamic reasons, the solid that grows in this case is made of two phases (called α and β) of different concentrations and crystal structures. The exchange of solute between the two phases during growth occurs by diffusion through the liquid. The proportion of the two phases in the solid is fixed by mass conservation, but their spatiotemporal arrangement along the front is a problem of nonlinear pattern formation [3,4]. It has been known for a long time that, within a certain range of values of the alloy concentration and V, the selected pattern is usually "lamellar" (periodic in one direction) and stationary (Fig. 1). This type of pattern (called "symmetrical" by contradistinction with the symmetry-broken patterns [5,6]) has a wide existence range as a function of the spacing λ at fixed V [7]. However, the nature of the predominant instability modes and the location of the instability thresholds on the λ scale are still largely open questions.

Most previous investigations of the stability of lamellar eutectic patterns were restricted to one-dimensional (1D) eutectic fronts. Quasi-1D fronts were obtained experimentally by using "thin" samples, i.e., samples of a thickness comparable to λ (on the order of 10 μm for V in the $\mu m\,s^{-1}$ range), in which the lamella plane is constrained to remain normal to the sample walls (but can undergo rotations about the normal to the sample plane). A transparent nonfaceted eutectic alloy (CBr_4-C_2Cl_6) was used, and the front was observed in real time through the wall of a glass container with a conventional optical microscope and a direction of observation normal to the wall [6]. These studies, in conjunction with numerical simulations, have led to the complete quantitative determination of the stability diagram of 1D eutectic fronts of CBr_4-C_2Cl_6 as a function of λ, V, and the alloy concentration [8–10]. In fact, this diagram obeys the so-called $\lambda V^{1/2}$ similarity law, meaning that the actual control parameter of the instabilities is $\lambda V^{1/2}$, or, equivalently, λ/λ_m, where λ_m is the so-called minimum-undercooling spacing, which is system dependent, and scales with V as $V^{-1/2}$ [7]. It was also shown numerically that the found qualitative features of the stability diagram were common to all nonfaceted binary eutectics.

When we turn to lamellar eutectics in bulk samples, we are faced with a new problem. In bulk samples, eutectic lamellae are not aligned along the normal to the sample walls—at least not quasi-instantaneously—contrary to what occurs in thin samples. They can rotate about the growth axis, and also break up, giving rise to topological

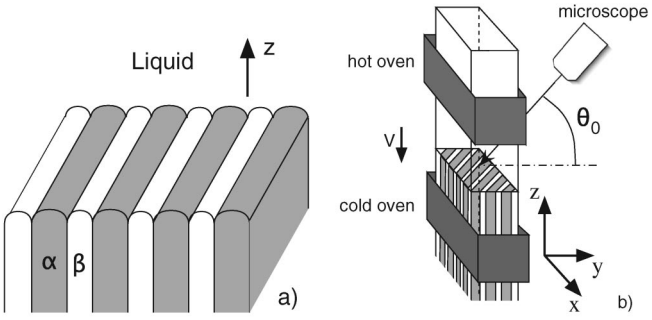

FIG. 1. (a) Sketch of a stationary lamellar eutectic pattern; α, β: eutectic crystal phases; **z**: axis of the thermal gradient, and normal to the growth front. (b) Sketch of the experimental setup; V: pulling velocity; θ_0: tilt angle of the direction of observation to the horizontal.

defects such as lamella terminations and line defects (domain boundaries and phase jumps). Moreover, numerous experiments have shown that, in bulk samples, lamellar patterns can disappear and be replaced by stationary patterns consisting of hexagonal arrays of inclusions of one phase embedded in the other (rodlike patterns) [7]. Thus, from the viewpoint of the phenomenological theories, 2D nonfaceted eutectic fronts can be characterized by the fact that they have, at fixed V, two types (lamellar and rodlike) of stationary patterns, which exist over finite-width spacing ranges, and are degenerate in orientation. These properties are shared by other 2D pattern-forming systems, in particular, Rayleigh-Bénard convection [11,12]. It is thus natural to try to find out if 2D lamellar eutectics exhibit the same primary mode of instability as Rayleigh-Bénard convection rolls do, namely, the zigzag instability. This question is currently being studied numerically [13,14] but has not yet been investigated experimentally.

In this Letter, we present real-time observations of 2D lamellar eutectic fronts in bulk samples of CBr_4-C_2Cl_6. The experimental setup is sketched in Fig. 1. We used 300- or 350-μm-thick glass samples filled with a slightly hypereutectic, well-purified alloy under a controlled atmosphere [15]. A thermal gradient of 100 ± 20 K cm^{-1} was installed between two isolated, temperature regulated copper blocks. The samples were equipped with a grain selector in order to grow single, or, at least, large, weakly anisotropic eutectic grains [16,17]. These were formed by using a procedure previously used in thin samples and described in Ref. [18]. The observations were performed in single-grain regions containing a hundred pairs of lamellae, typically. We checked that the isotherms were planar and perpendicular to z (to within 1°) when the sample was at rest. However, a small ($< 6°$) tilt of the isotherms about the x axis (thermal bias) sometimes occurred during solidification. The presence of convection flows with velocities of a few 10 μm s^{-1} was also revealed by a lateral drift of small inert dust particles floating in the liquid close to the front, though the system is, in principle, stable against thermosolutal convection in hypereutectic CBr_4-C_2Cl_6 alloys—the liquid close to the front is enriched in CBr_4, which is denser than C_2Cl_6. We did not detect any perturbation due to these flows in the regions of the samples in which the observations were performed.

The front was observed from the top through the liquid and a lateral glass plate of the container. The contrast arises from the differences of optical index between the three transparent phases. A major difficulty was to separate the image of the growth front from that of the underlying two-phase solid. We solved this problem by choosing a dark-field method, in which the directions of observation and lighting are both oblique, but different from each other. We used a long-distance microscope (Questar QM100) with large working distance (15 cm) and depth of field ($\simeq$200 μm). The light source was made of a halogen lamp and a linear bundle of optic fibers. The images were captured with a video camera and then digitized and filtered numerically for contrast enhancement. The reduction of the image in the y direction due to the oblique direction of observation was also corrected numerically. We fixed the tilt angle of the direction of observation at 50°, which corresponds approximately to the minimum value (2.85) of the image reduction factor along the y axis. [The existence of a minimum is due to the refraction of the light at the liquid-(glass)-air interface.] A corrected image of a quasistationary lamellar pattern is shown in Fig. 2. A sharp, almost uniform, optical contrast between (bright) β and (dark) α lamellae is obtained. The shape of the front on a scale smaller than λ is not resolved, but this was not necessary for our purpose.

We have performed solidification runs over long periods of time (several hours) for various values of the alloy concentration and V. Most generally, the pattern obtained at the end of the initial transient (about 10 min after the onset) was quite complex and showed no preferred orientation of the lamella plane, except near the sample walls, where the no-flux condition forces the lamellae to be normal to the walls (Fig. 3). In general, a pronounced alignment normal to the sample walls was obtained after a long time through a progressive elimination of the topological defects and a slow propagation of the wall effect across the sample. The dynamics of this relaxation toward a stationary state will be reported elsewhere. In most samples, the relaxation process led to a pattern that was essentially a symmetrical one, despite the persistence of a few undulations and lamella terminations that were probably due to imperfections of the experimental setup, such as thermal bias, long-range concentration gradients in the liquid, convection flows, and grain boundaries (Fig. 2). In a few samples, however, the final stationary pattern was clearly of the zigzag type [Fig. 4(a)]. This

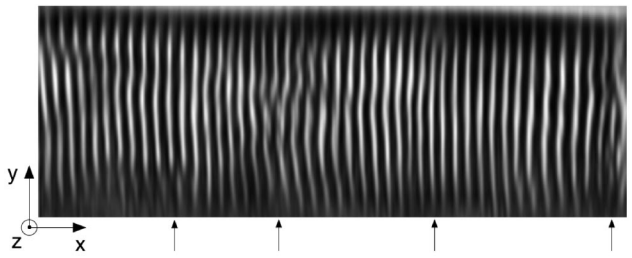

FIG. 2. Top view of a symmetric lamellar eutectic pattern in a 350-μm-thick sample of a slightly hypereutectic CBr_4-C_2Cl_6 alloy. $V = 0.37$ μm s^{-1}. The sample was pulled at $V = 0.5$ μm s^{-1} for 4.5 h and then at 0.37 μm s^{-1} for 1.5 h. Bright and dark stripes are β and α lamellae, respectively. Horizontal width of the image: 860 μm. Average value of λ: $0.82\lambda_m$. Arrows: lamella terminations.

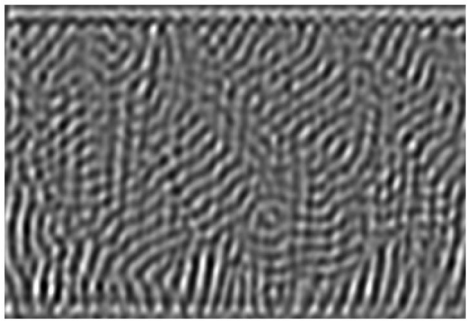

FIG. 3. View of a pattern after 10 min at $V = 0.5\ \mu\mathrm{m\,s^{-1}}$, and 35 min at $V = 1\ \mu\mathrm{m\,s^{-1}}$ in a 300-μm-thick sample. Lamellar domains are separated by disordered regions containing topological defects, and rods. Horizontal width 440 μm.

was due to the fact that the average spacing of the system was larger than usual in these experiments (see below), but the reason of this fact itself (the larger average spacing) was unclear, except that it occurred only in samples in which the experimental imperfections happened to be particularly weak.

The transition from symmetrical to zigzag patterns was studied as follows. An almost uniform zigzag pattern was obtained in a large (about 1-mm wide) eutectic grain after a 4 h pulling at $V = 0.5\ \mu\mathrm{m\,s^{-1}}$. It was then submitted to a sequence of four V jumps separated by 30 min pullings at constant V. We first decreased V to 0.39 and $0.3\ \mu\mathrm{m\,s^{-1}}$ and then reincreased it to 0.39 and $0.5\ \mu\mathrm{m\,s^{-1}}$. The first three steps of the sequence are illustrated in Fig. 4. We extracted the local values of λ, the amplitude A, and the wavelength L of the zigzag modulation by fitting the skeletonized image of the lamellae with a sine function over some space periods in different regions of the micrographs. We assumed that the control parameter of the instability is λ/λ_m, as it is for the 1D instabilities. The measured values of A and L are plotted as a function of λ/λ_m in Fig. 5. Despite the dispersion of the data, it is clear that there exists a threshold λ_c, located between $0.85\lambda_m$ and $0.95\lambda_m$, below which no zigzag pattern was observed, and above which A increased as λ/λ_m increased. This is a clear sign of a bifurcation, although the character (supercritical or slightly subcritical) of this bifurcation could not be determined. The existence of a region without zigzags at the lowest values of V in Fig. 4 does not necessarily mean that the bifurcation was subcritical. The zigzag pattern actually exhibited a slow global (upward) drift along the y axis, at a velocity v_d of about $0.05\ \mu\mathrm{m\,s^{-1}}$ for $V = 0.5\ \mu\mathrm{m\,s^{-1}}$. Most probably, this was not an intrinsic property of the pattern, but the consequence of a thermal bias, which was comparable to $\tan^{-1}(v_d/V) = 5.7°$ in this experiment. This external forcing can explain the persistent absence of zigzags up to a certain distance (which increases as $\lambda - \lambda_c$ decreases) from the colder wall, as observed in Figs. 4(b) and 4(c). Finally, Fig. 5(b) shows that L steeply increased when V was diminished and redecreased with some hysteresis as V was switched back to its initial value. This is a characteristic behavior of the zigzag instability, as studied, for instance, in Rayleigh-Bénard convection, which originates from its "diffusive" character, i.e., from the fact that its amplification coefficient ω and wave vector k are related by $\omega = -D(\mu)k^2$ at small k, where $\mu = (\lambda - \lambda_c)/\lambda_m$ is the dis-

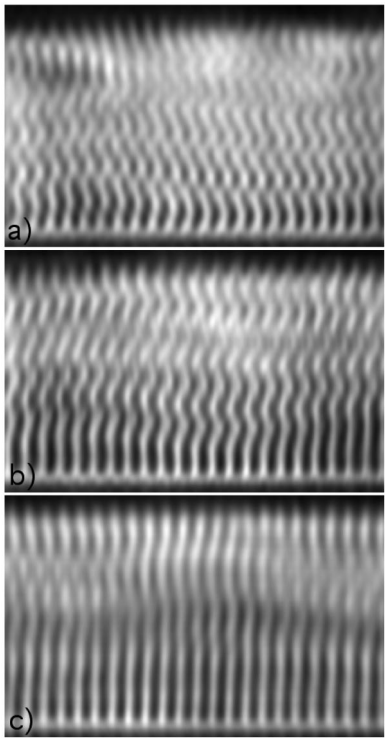

FIG. 4. Top views of zigzag patterns (a) $V = 0.5\ \mu\mathrm{m\,s^{-1}}$. Solidification time: 4 h; (b) $V = 0.39\ \mu\mathrm{m\,s^{-1}}$. Solidification time: 30 min; (c) $V = 0.3\ \mu\mathrm{m\,s^{-1}}$; solidification time: 30 min. Sample thickness 300 μm. Horizontal width 440 μm.

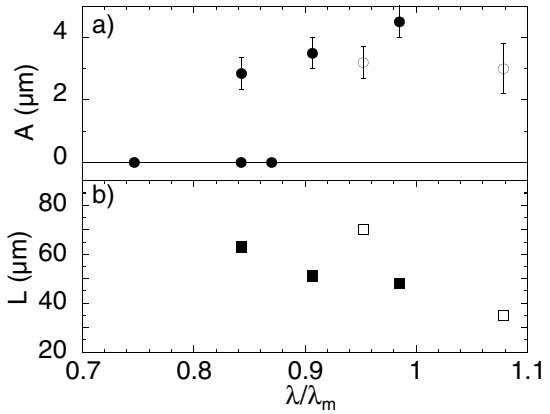

FIG. 5. (a) Amplitude A and (b) wavelength L of the zigzags vs the reduced spacing λ/λ_m. Filled (open) symbols: data obtained by decreasing (increasing) V. The error bars represent the experimental dispersion.

tance from the instability threshold, and $D(\mu)$ (phase diffusion coefficient) changes sign at $\mu = 0$ [12]. In conclusion, our observations prove the existence of a zigzag bifurcation, the threshold of which corresponds to the upper stability bound of the symmetric lamellar patterns, in bulk near-eutectic CBr_4-C_2Cl_6.

We have also studied the lower (upper) stability bounds of the symmetrical (zigzag) patterns. The symmetrical patterns were unstable against lamella elimination below about $0.7\lambda_m$—as they are in thin samples [10]—while the zigzag patterns were unstable against a lamella breakup instability above about $1.1\lambda_m$. The lamella breakups generally evolved into the creation of new lamellae, which reduced the spacing. We never observed any lamellar pattern with a value of λ/λ_m lying outside the range 0.7–1.1, even in small domains. It is thus clear that the morphology diagram of nonfaceted eutectics in bulk samples is profoundly different from what it is in thin samples. In thin samples, the zigzag and the lamellar breakup are usually blocked allowing a series of symmetry-breaking (tilt and oscillations) bifurcations to occur at spacings larger than $1.1\lambda_m$ [8,9]. In bulk samples, the occurrence of the lamella breakup at relatively small spacings eliminates these bifurcations and leads to the formation of topological defects. We have observed that, sufficiently far above the threshold, the zigzag patterns always exhibited line defects corresponding to a phase jump of the pattern. Such a defect extending over about 10λ can be seen at the bottom of Fig. 4(a). In this particular case, the defect disappeared when we decreased V, indicating that it was not linked to a subboundary in the crystals but was an intrinsic nonlinear property of the zigzag pattern. This may be a clue to the origin of the "line faults" or "mismatch surfaces" that always appear in large density in the cross- sections of bulk metallic lamellar eutectics [19]. Our observations suggest that such "faulty" patterns might be steady at spacings much larger than the zigzag instability threshold. This would be compatible with the fact that the λ distributions measured in bulk metallic eutectics generally have a larger width ($>20\%$) [20] than that of the stability range of the symmetrical lamellar pattern ($\simeq 10\%$).

In conclusion, the experimental setup that we have presented here is a powerful tool for the study of eutectic growth patterns in bulk samples. It has allowed us to show that a zigzag bifurcation is the primary instability of a bulk lamellar eutectic (CBr_4-C_2Cl_6) near the eutectic concentration and that this bifurcation occurs at an unexpectedly low ($0.85\lambda_m$) spacing value. A similar result was recently found numerically using a phase-field method and a one-sided model (no diffusion in the solid) by Parisi and Plapp [13]. The investigation of other aspects of 2D eutectic growth, such as the dynamincs of line defects, the lamella-rod transition, and the effects of the convection flows, is in progress.

We thank M. Plapp and A. Parisi for many fruitful discussions and for communicating their unpublished numerical results. We gratefully acknowledge the technical help of C. Perez and C. Picard. This research was financially supported by the Centre National d'Etudes Spatiales, France.

*Electronic address: bottin@gps.jussieu.fr

[1] M. C. Cross and P. C. Hohenberg, Rev. Mod. Phys. **65**, 851 (1993).
[2] *Proceedings of Solidification Processes and Microstructures: A Symposium in Honor of W. Kurz*, edited by M. Rappaz, C. Beckermann, and R. Trivedi (TMS, Warrendale, 2004).
[3] J. S. Langer, Phys. Rev. Lett. **44**, 1023 (1980); V. Datye and J. S. Langer, Phys. Rev. B **24**, 4155 (1981).
[4] A. Karma, Phys. Rev. Lett. **59**, 71 (1987).
[5] K. Kassner and C. Misbah, Phys. Rev. A **44**, 6513 (1991).
[6] G. Faivre and J. Mergy, Phys. Rev. A **45**, 7320 (1992).
[7] K. A. Jackson and J. D. Hunt, Trans. Metall. Soc. AIME **236**, 1129 (1966).
[8] A. Karma and A. Sarkissian, Metall. Trans. A **27**, 635 (1996).
[9] M. Ginibre, S. Akamatsu, and G. Faivre, Phys. Rev. E **56**, 780 (1997).
[10] S. Akamatsu, M. Plapp, G. Faivre, and A. Karma, Phys. Rev. E **66**, 030501(R) (2002); Metall. Mater. Trans. A **35**, 1815 (2004).
[11] F. H. Busse, Rep. Prog. Phys. **41**, 1929 (1978)
[12] P. Manneville, *Dissipatives Structures and Weak Turbulence* (Academic Press, Boston, 1990).
[13] A. Parisi and M. Plapp (unpublished).
[14] A. Karma and M. Plapp, JOM **56**, No. 4, 28 (2004).
[15] J. Mergy, G. Faivre, C. Guthmann, and R. Mellet, J. Cryst. Growth **134**, 353 (1993).
[16] B. Caroli, C. Caroli, G. Faivre, and G. Mergy, J. Cryst. Growth **118**, 135 (1992).
[17] G. Faivre, in Ref. [2], p. 239.
[18] S. Akamatsu, S. Moulinet, and G. Faivre, Metall. Mater. Trans. A **32**, 2039 (2001).
[19] D. D. Double and A. Hellawell, Philos. Mag. **19**, 1299 (1969); J. P. Riquet and F. Durand, Mater. Res. Bull. **10**, 451 (1973); H. Dean and J. E. Gruzleski, J. Cryst. Growth **21**, 51 (1974).
[20] R. Trivedi, J. T. Mason, J. D. Verhoeven, and W. Kurz, Metall. Trans. A **22**, 252 (1991).